This article has been accepted for publication in a future proceedings of this conference, but has not been fully edited.
Content may change prior to final publication. Citation information: DOI 10.1109/THERMINICXXXXX.2022.XXXXXXX, 2022 28th International Workshop on Thermal Investigations of ICs and Systems (THERMINIC) Proceedings **Therminic 2022**

Review on Flow Boiling Patterns in Microchannels

Joseph Widgington
Centre for Energy Efficient and Sustainable Technologies
Department of Mechanical and Aerospace Engineering, Brunel University London
London, United Kingdom
Joseph.Widgington@brunel.ac.uk

Atanas Ivanov
Centre for Energy Efficient and Sustainable Technologies
Department of Mechanical and Aerospace Engineering, Brunel University London)
London, United Kingdom
Atanas.Ivanov@brunel.ac.uk

Tassos Karayiannis
Centre for Energy Efficient and Sustainable Technologies
Department of Mechanical and Aerospace Engineering, Brunel University London
London, United Kingdom
Tassos.Karayiannis@brunel.ac.uk

***Abstract*— A discussion on the current challenges that face the heat transfer community in predicting two-phase flow patterns in microchannels is presented in this paper. These challenges include lack of universal terminology, a requirement for an agreed flow pattern categorisation by the international research community and subjectivity due to visual categorisations of flow patterns. The generic flow pattern categorisation of bubble, slug, churn and annular flows are suggested to alleviate these problems. Finally, a data bank consisting of over 1500 data points for a range of fluids was used to assess the success of current diabatic flow pattern transition models and to understand the important parameters that cause flow patterns to transition.**

Keywords— Flow Boiling, Flow Patterns, Two-Phase Flows

NOMENCLATURE

Bo	Boiling number [-] $Bo = \frac{q"}{Gh_{fg}}$
Co	Confinement number [-] $Co = \frac{1}{D_h}\sqrt{\frac{\sigma}{g(\rho_l - \rho_g)}}$
D_b	Bubble departure diameter [m]
D_h	Hydraulic diameter [m]
F	Force [N]
Fr	Froude Number [-] $Fr = \frac{G^2}{\rho_l{}^2 g D_h}$
G	Mass flux [kg/m^{2}s]
g	Gravitational constant [m/s^2]
h_{fg}	Latent heat of vaporisation [J/kg]
MAE	Mean absolute percentage error [-]
n	Number of data points
$q"$	Heat flux [W/m^2]
Re	Reynolds numer [-] $Re = \frac{GD_h}{\mu}$
U	Velocity [m/s]
We	Weber numer [-] $We = \frac{G^2 D_h}{\rho\sigma}$
x	Vapour quality [-]

Greek Symbols

α_c	Critical void fraction [-]
θ	Contact angle [rad]
μ	Viscosity [kg/ms]
ρ	Density [kg/m^3]
σ	Surface tension [N/m]

Subscript

act	Actual values
by	Bouyancy
g	Gas/ vapour
i	Inertia
l	Liquid
p	Evaporation momentum
$pred$	Predicted values
s	Superficial
μ	Viscous
σ	Surface tension

I. INTRODUCTION

There has been a meteoric development in microprocessor design in the last forty years that has resulted in an exponential rise in processing power per chip footprint area [1]. As such, significantly higher heat fluxes are being generated due to proportionally higher power leakages over the reduced die footprint. The heat fluxes being generated by modern microprocessors have now reached over 10 MW/m², thus rendering traditional air-cooled methods insufficient for the current cooling requirements that microprocessors present [2]. The efficient thermal management of microprocessor devices dictates that operating temperatures are contained to below 85 ºC in consumer electronics and 175 ºC in more advanced limited silicon-based devices [3]. Consequently, there has been a sharp rise in the research of novel cooling solutions, where two-phase flow boiling in microchannel heat sink devices proved to be one of the most promising techniques [4]. It is now necessary to conclude on the predictive tools for heat transfer rates and pressure drop in these devices in order to increase general adoption by industry.

Heat and mass transfer processes in flow boiling are intrinsically linked to the characteristic flow patterns that develop at the interface between the liquid and vapour phases. For example, the nucleate heat transfer mechanism enhances heat transfer through increased agitation and mixing of the bulk fluid when bubbles depart from the heated surface. The nucleate heat transfer mechanism is therefore more dominant when the bubble flow regime is prevalent [5]. Alternatively, the convective heat transfer mechanism is enhanced when an increased vapour inertial force is present at the liquid-vapour interface and when the liquid film thickness at the channel wall is reduced. This heat transfer mechanism is believed to be dominant in the annular flow regime [6]. The parametric effect on heat transfer coefficients is notably different between the two mechanisms. An increased heat flux results in a greater nucleation site density in the nucleate boiling mechanism, causing greater liquid agitation and improved heat transfer performance [7]. There is an insignificant mass flux effect on heat transfer coefficient in the nucleate boiling mechanism. Increasing the mass flux parameter will increase the vapour inertial force, resulting in in thinning of the liquid film. Accordingly, increased mass flux enhances the heat

This article has been accepted for publication in a future proceedings of this conference, but has not been fully edited.
Content may change prior to final publication. Citation information: DOI 10.1109THERMINICXXXXX.2022.XXXXXXX,
2022 28th International Workshop on Thermal Investigations of ICs and Systems (THERMINIC) Proceedings **Therminic 2022**

transfer performance in the convective heat transferor mechanism and there is a negligible heat flux effect.

Most of the past modelling of parametric effects on heat transfer rates across the full range of flow patterns relied solely on semi-empirical fits of data without knowledge of the dominant flow patterns [8] and with applicability that is limited to within the range of the data bank used. In addition, there are few comprehensive flow pattern maps for microscale flows, where it is agreed that the modifications of flow pattern transition models that exist for conventional channels provide poor predictions of transitions in the microscale [9]. Moreover, the small number of current flow pattern maps and models/correlations for determining flow pattern transitions are often limited to particular operating conditions and for a given fluid [5]. These limitations act as a further barrier to their administration as prediction tools in industrial applications of microscale heat exchangers, where operation with new and novel fluids may be required.

Attempts to develop universal flow pattern maps are also hindered by an apparent disagreement between the reported flow patterns in the microscale, even when similar operational parameters and fluids are used. Two potential reasons for flow pattern discrepancies include: (1) the subjectivity in categorising flow patterns that arises due to visual observation techniques [10] and (2) the lack of universal terminology that exists when describing flow patterns in the microscale [11]. The work presented here aims to elucidate the generally accepted universal microscale flow pattern designations that would help eliminate the above two issues and help determine the mechanisms upon which the transitions to each designated flow pattern is dependent. The resultant conclusions in this work will contribute to the understanding of prevailing heat transfer mechanisms and help researchers propose phenomenological correlations for heat transfer rates and pressure drop in microchannel heat exchangers.

II. FLOW PATTERNS IN THE MICROSCALE

Classifications of two-phase flow patterns present disagreements between publications, even in conventional sized channels. A disparity has developed between researchers that desire an exhaustive set of flow pattern designations and others that deem the differences between some flow pattern designations to be insignificant in the application of engineering design. However, it is mainly agreed between researchers that the four main flow pattern categorisations are stratified, bubble flow, intermittent flow and annular flow. The four main flow regimes are often further subdivided and additional transitional categorisations used. Fig. 1 depicts the four main flow pattern categorisations and the further subdivisions of elongated bubble, slug, churn, smooth stratified and wavy stratified flows.

Observed flow patterns vary between flow orientations in conventional sized channels. Stratified, bubble, elongated bubble, slug and annular flows are observed in horizontal channels, whilst bubble, elongated bubble, slug, churn and annular flows are seen in vertical channels. The forces that act on the liquid vapour interfaces in two-phase flows can explain this phenomenon. These forces are the inertial force, surface tension force, viscous force, buoyancy force and evaporation momentum force. Kandlikar [12] scaled the five forces with respect to unit area, see Table I, by dividing the resultant force magnitudes by the square of the characteristic length so that their effects can be seen on flow patterns, heat transfer rates and flow instabilities in two-phase flows. The buoyancy force vector alters in direction with channel orientation, acting parallel to the flow direction in vertical channels and perpendicular in horizontal channels. Stratified flow occurs due to the separation of the vapour and liquid flows as a consequence of the buoyancy force. This separation can only occur if the buoyancy force, or a component of it, acts perpendicular to the flow direction and hence, stratified flow cannot exist in conventional vertical channels.

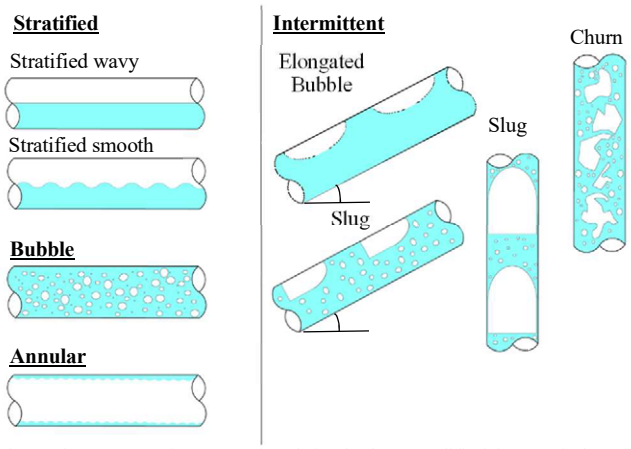

Fig.1. Flow patterns in conventional sized tubes (modified from Taitel [13]).

TABLE I. REVEVANT FORCES SCALED PER UNIT AREA.

Inertia Force	Surface Tension Force	Viscous Force	Bouyancy Force	Evaporation Momentum Force
$F_i = \frac{G^2}{\rho}$	$F_\sigma = \frac{\sigma}{D_h}$	$F_\mu = \frac{\mu G}{\rho D_h}$	$F_{by} = (\rho_l - \rho_g) g D_h$	$F_p = \frac{\left(\frac{q''}{h_{fg}}\right)^2}{\rho_g}$

Flow pattern observations in the microscale differ significantly from those in conventional channels, especially for horizontal flows. The differences in observed flow patterns has been used to define the demarcation between macro and microscale in two-phase flows. Two observations that are commonly made in two-phase horizontal microchannel flows are a uniform (or near uniform) annular flow film thickness and the absence of stratified flow. The scaled forces presented in Table I show that the buoyancy force decreases with a reduced hydraulic diameter but the viscous and surface tension forces increase with a reduced hydraulic diameter. The buoyancy force therefore becomes sufficiently suppressed in small geometries so that a full separation of the vapour phase to the top of the channel cannot occur. Furthermore, the buoyancy force in conventional channels acts to reduce the liquid film thickness at the top of the channel in comparison to the bottom. This phenomenon does not occur in microchannels due to the reduced scaled buoyancy force.

As mentioned above, researchers have used these two flow pattern phenomena as a method of quantitively defining the microscale. Ong and Thome [9] used liquid film thickness measurements to formulate the microscale threshold criterion presented in (1) which occurs when the buoyancy forces are sufficiently weak. Tibiriçá and Ribatski [13] also defined the microscale on the basis of buoyancy force. Equation (2) was presented to define where the scaled buoyancy force is less than 5% of the scaled surface tension force, producing a near uniform film thickness. A second criterion was also presented by Tibiriçá and Ribatski where a force balance was conducted on a vapour plug which would form in the absence of stratified

This article has been accepted for publication in a future proceedings of this conference, but has not been fully edited.
Content may change prior to final publication. Citation information: DOI 10.1109/THERMINICXXXXX.2022.XXXXXXX,
2022 28th International Workshop on Thermal Investigations of ICs and Systems (THERMINIC)

flow, i.e. a mechanistic criterion in which stratified flow will not exist. The definition of microscale used in this study is the hydraulic diameter at which stratified flow no longer exists in horizontal flows due to suppression of the buoyancy forces.

$$Co = \frac{1}{D_h}\sqrt{\sigma/[g(\rho_l - \rho_g)]} > 1 \quad (1)$$

$$D_h < \sqrt{\sigma/[20g(\rho_l - \rho_g)} \quad (2)$$

The appearance of churn flow in horizontal microchannels is another phenomenon that is commonly reported in literature. As an example, recent experiments by Lee and Karayiannis [14] and Al-Zaidi et al. [15] on flow boiling in horizontal multi-channel microscale heat sinks both reported churn flow, images of which are displayed in fig. 2. The lack of stratified flow and appearance of churn flow in horizontal microchannels results in the classifications of flow patterns between vertical and horizontal microchannels being identical. Referring back to fig. 1 and the classifications of Taitel [13], it can be concluded that the flow patterns in microchannels include bubble, intermittent and annular flow patterns. In this case, intermittent includes elongated bubble, slug and churn flows.

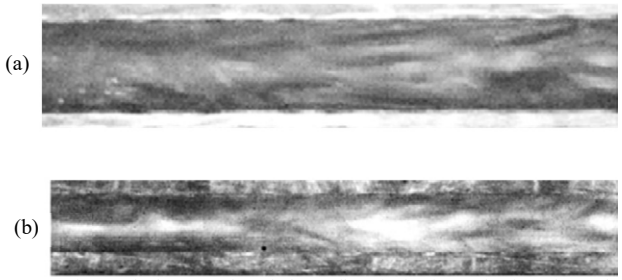

Fig.2. Experimental photographs of churn flow in horizontal microchannels from (a) Lee and Karayiannis [16] and (b) Al-Zaidi et al. [17].

Chen et al. [18] developed detailed flow pattern models for small vertical tubes using classical flow pattern categorisations. The flow patterns observed by Chen et al. are presented in fig. 3 under the classification of dispersed bubble, bubble, confined bubble, slug, churn and annular flows. Dispersed bubble is a subdivision of bubble flow where small, spherical bubbles exist with a flow velocity similar to that of the liquid phase. This differs from conventional bubble flow, where larger, bubbles of a less spherical shape travel with a velocity lower than that of that of the liquid phase.

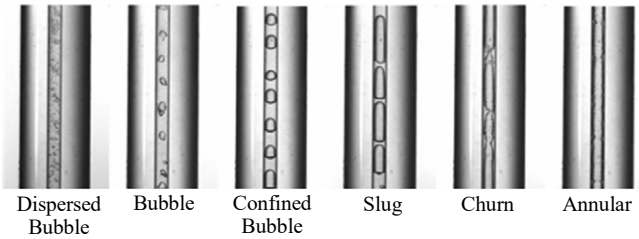

Fig. 3. Observed flow patterns in a 1.1 mm vertical tube (adapted from Chen et al. [18])

These classical designations of flow patterns are commonly used by many authors however, variations in terminology often exists between publications. For example, Thulasidas et al. [19] reported a flow pattern as bubble-train flow which Damianides and Westwater [20] referred to as plug flow. The flow patterns reported here are identical to the slug flow pattern that is evident in fig. 3. Furthermore, additional subdivided transitional categorisations and terminologies have been used in an attempt to determine an exhaustive description of microscale flow patterns. One example of this would be wavy-annular flow by Coleman and Garimella [21], which has also been referred to as pseudo-slug flow by Fan et al. [22]. Coleman and Garimella reported that the flow pattern occurred between stratified flow and annular flow, where a wavy, unstable interface occurred. The microscale has been defined as geometry in which stratified flow cannot exist in this study and hence, Coleman and Garimella's wavy-annular flow would not exist in microchannels. However, the classification of wavy-annular flow has also been used to describe a flow pattern in which the interface between the liquid and vapour phases in annular flow becomes unstable, causing a wave like structure to the interface. A photographic image and diagrammatic explanation of this flow pattern is displayed in fig. 4 (a) from Habibi and Moghaddam [23]. A clear vapour core with a film thickness that is near uniform at a given location along the channel is evident in this definition of wavy-annular flow. However, fig. 4 (b) depicts a photographic image of Coleman and Garimella's wavy-annular flow and shows near full separation of the liquid and vapour phases with the vapour phase almost entirely at the top of the channel. Therefore, whilst Coleman and Garimella's wavy annular flow would not exist in microchannels, Habibi and Maghaddam's wavy-annular flow does.

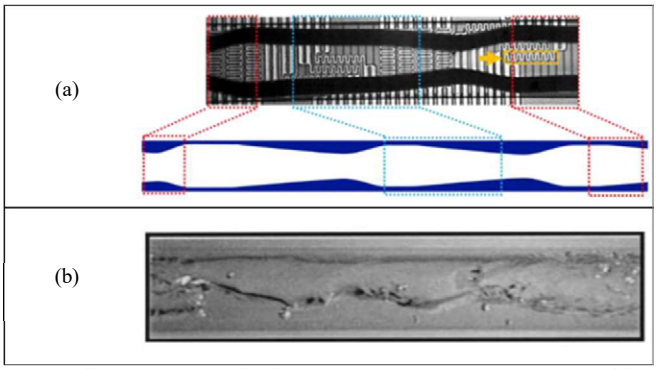

Fig. 4. Differing wavy-annular flow pattern categorisations (a) from Habibi and Moghaddam [23] and (b) from Coleman and Garimella [21].

Currently, there are no universal prediction tools that are capable of accurately predicting the fundamental flow pattern transitions in microchannels. Accordingly, the designation and prediction of transitional flows must be a secondary focus to the development of correlation models of the fundamental generic flow patterns. A solution to the issue of the lack of universal terminology is to adopt the generic categorisations of dispersed bubble, bubble, elongated bubble, slug, churn and annular flows, as described by Chen et al. [18].

Flow patterns are often observed using high speed recording devices and then visually categorised by researchers. Thus, a problem of visual subjectivity may still be an issue if the designations of Chen et al. are utilised. Revellin and Thome [24] attempted to eliminate this problem by using quantitative measurements for bubble generation frequency, as shown in fig. 5. The data was divided into three trends namely: (1) where the bubble count frequency increased with increasing vapour quality (2) where the bubble count frequency decreased with increasing vapour quality and (3) where the bubble count frequency reached zero. The first trend was described as the isolated bubble regime, the second as the coalescing bubble regime (as the reduction in in bubble count frequency was deemed to be due to the coalescence of bubbles) and the third was the annular flow regime (where bubble nucleation has become suppressed by a liquid film)

This article has been accepted for publication in a future proceedings of this conference, but has not been fully edited.
Content may change prior to final publication. Citation information: DOI 10.1109THERMINICXXXXX.2022.XXXXXXX,
2022 28th International Workshop on Thermal Investigations of ICs and Systems (THERMINIC)

he methodology outlined by Revellin and Thome [24] and used in subsequent publications (see [9], [25]) is successful in eliminating the subjectivity that arises due to visual observations. However, there may exist the inability to determine the dominant heat transfer mechanisms in each flow pattern categorisation. For instance, the reduction in bubble count frequency due to the coalescence of bubbles in the coalescing bubble regime may still result in bubbles with diameters less than that of the channel, i.e. they are not confined. In this case nucleate boiling will still be dominant. Alternatively, the bubbles may be coalescing to form vapour slugs in the coalescing bubble regime which replicates the classical designation of elongated bubble flow. Thome et al. [26] previously devised a mechanistic three-zone heat transfer model that found nucleate boiling not to be a dominant heat transfer mechanism when elongated bubble flow is the dominant flow pattern in microchannels. Furthermore, the chaotic nature of churn flow is not captured in these three categorisations, resulting in a future inability to mechanistically determine heat transfer rates and pressure drops for this flow pattern.

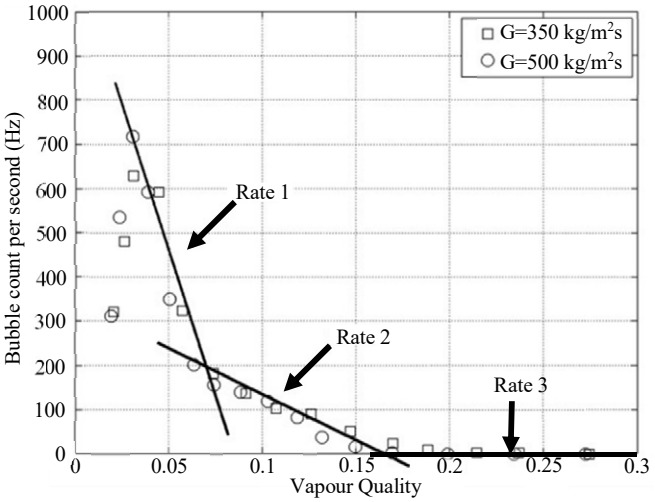

Fig. 5 Bubble count verses vapour quality (modified from Revellin and Thome [24].

It is therefore logical that the classical terminology, such as those used by Chen [18], is implemented so that the dominant heat transfer mechanisms can be clearly recognised. However, it is important to use classifications that will eliminate visual subjectivity and it should be noted that transitions between flow patterns are gradual. The distinction between dispersed bubble and bubble flow is difficult to determine as the two main differences, in addition to the bubble size, are the velocity of the bubbles in reference to the liquid phase and the geometry of the bubble. Whilst in dispersed bubble flows the velocity is similar to that of the liquid phase, there will always be some slippage between phases. Secondly, whilst the bubbles are more spherical in dispersed bubble flow, they again are not perfectly spherical. It is therefore not feasible to determine when the velocity of the bubble is significantly disparate to that of the liquid, or for the three-dimensional sphericity of the bubble to be accurately determined to provide a definitive quantitative transition from dispersed bubble to bubble flow. Furthermore, the dominant heat transfer mechanism in both flow pattern categorisations is the nucleate boiling mechanism. Hence, it is recommended that the dispersed bubble and bubble flow patterns are merged into a single flow pattern categorisation.

Two additional flow patterns that pose a difficulty in determinine a clear difference through visual observation are elongated bubble flow and slug flow. Confined bubble flow contains bubbles that have a spherical cap and bottom due to confinement of the bubble by the channel wall. Conversely, slug flow conntains “bullet” shaped vapour slugs due to the bubble becoming distorted by the wall restrictions. Once again, it is hard to quantify the degree to which a vapour bubble is either spherical or bullet shaped, thus creating subjectivity when defining the transition. In addition, the heat transfer mechanism for both elongated bubble and slug flows are very similar, both being a transient phenomenon due to the periodic passing of the liquid and vapour phases across a single point on the channel, requiring a time averaged steady state heat transfer coefficient to be obtained [26]. Accordingly, the amalgamation of elongated bubble and slug flows into the single categorisation of slug flow will also reduce the subjectivity in defining flow patterns.

Thus, the logical categorisation of flow patterns to allow full understanding of the heat transfer mechanisms, eliminate problems with a lack of universal terminology and subjectivity are:

Bubble flow: bubble diameter is less than that of the channel

Slug flow: bubble diameter is equal to that of the channel and will then begin to elongate

Churn flow: The vapour-liquid interface at the nose or tail of the bubble has become unstable so that no clear interface line can be seen. Separation of the phases is not complete and there is no vapour core.

Annular flow: The phases have full separated so that there is a liquid film on the surface of the channel and a vapour core in the centre

III. Microscale Flow Pattern Maps

Numerous flow pattern transition models have been proposed to predict the prevailing flow patterns in microchannels for a given geometry, fluid and operating conditions. Such predictive tools have been developed through a variety of experimental techniques that can be divided into three categories. The first category can be classified as the adiabatic methodology, where two-phase flows are established by injecting a gas into a liquid flow with no heating. The two-phase flow pattern is then observed and categorised in a viewing part of the test section. The limitation of this methodology is that it does not account for the effect of heat flux on the two-phase flow patterns and neglects the evaporation momentum force. Subsequently, this experimental methodology may not truly reflect the prevailing flow patterns in microscale heat exchangers. The second category is the indirect diabatic methodology, in which two-phase flows are produced by heating single phase liquid in part of the test section, while flow patterns are observed and categorised in a viewing part of the test section, as shown in fig. 6 which depicts a typical indirect diabatic test section. This allows for the inclusion of the effect of heat flux and evaporation momentum force when categorising flow patterns, unlike the adiabatic technique. It can also utilise direct electrical heating to enable a reasonable range of heat flux to be studied compared to, for example, transparent passages coated with an electrically contacting material. Finally, in the direct diabatic methodology heating is applied and flow visualisation is conducted over the heated area of the

This article has been accepted for publication in a future proceedings of this conference, but has not been fully edited. Content may change prior to final publication. Citation information: DOI 10.1109THERMINICXXXXX.2022.XXXXXXX, 2022 28th International Workshop on Thermal Investigations of ICs and Systems (THERMINIC)

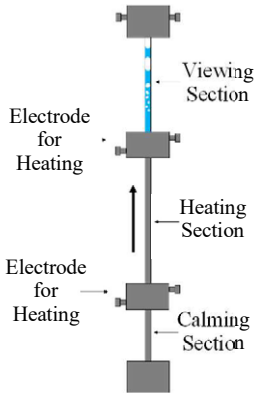

Fig. 6. Diagram of typical indirect diabatic test section (modified from Chen et al. [18]

test section. Visualisation of flow in a section that is also heated results in observation of flow patterns that would directly represent those that are present in microchannel heat exchangers. This has an advantage over the indirect diabatic methodology, where flow is only visualised downstream of the heated section, which may result in bubble coalescence in the viewing section and a differing flow pattern observed. Thus, care must be exercised when comparisons between heat transfer rates and prevailing flow patterns are made. For example, it has been shown that increased bubble generation in the bubble regime will increase agitation and thus, heat transfer rates [27], these bubbles may coalesce downstream in the viewing section and result in slug flow being observed and categorised. In the described case, the heat transfer results obtained in the heating section would be high, whilst slug flow has actually been found to reduce heat transfer rates [17]. The data and correlations used for comparisons in this study were obtained or developed through experiments using the indirect or direct diabatic techniques. Whilst the indirect diabatic methodology can have the aforementioned limitation, there is limited flow pattern data obtained solely through the direct diabatic methodology to feasibly analyse flow pattern prediction tools.

Flow pattern correlations and predictive methods are typically presented using flow pattern maps. The co-ordinate system of each map can vary between publications but typical systems include superficial gas velocity, superficial liquid velocity, vapour quality, and mass flux. Coordinate systems have included the use of dimensionless parameters such as Boiling numbers, Eötvos numbers, Reynolds numbers and Weber numbers. Whichever co-ordinate system has been selected, each transition boundary line is designed to best reflect the relevant parameters that result in the transition between flow patterns. However, the use of different coordinate systems makes it difficult to compare transition correlations between publications. Therefore, in this paper each set of flow pattern transition correlations has been plotted on a coordinate system where superficial gas velocity is the abscissa and superficial liquid velocity the ordinate.

A large flow boiling data bank based on observations of past studies for two-phase horizontal single-channels, horizontal multichannels and vertical single tubes is now available in Centre for Energy Efficient and Sustainable Technologies at Brunel University London. A set of over 1500 data points was compiled for these studies, for either direct or indirect diabatic experiments. The data were compared to five current transition models, which are displayed in Table II (see [8], [9], [18], [24], [28] for a complete set of correlations). The classifications of isolated bubble, coalescing bubble and annular flows were compared to classical designations. As such, the isolated bubble to coalescing bubble transition boundary was classified as a bubble to slug transition and the coalescing bubble to annular flow transition was classified as a churn to annular transition.

TABLE II. COMPARED FLOW PATTERN MODELS

Authors	Fluid(s) used	D_h(mm)	Methodology
Chen et al. [18]	R134a	1.1 – 4.26	Indirect Diabatic
Mahmoud and Karayiannis [8]	R245fa	1.1	Indirect Diabatic
Revellin and Thome [24]	R134a, R245fa	0.509-0.790	Indirect Diabatic
Ong and Thome [9]	R134a, R236fa, R245fa	1.03-3.04	Indirect Diabatic
Tibiriçá et al. [28]	Bubble-Slug: Air-water, R134a, R245fa, R236fa, R1234ze(E) Slug-Churn: Nitrogen, R134a, R245fa, R123ze(E) Churn-Annular: Air-water, Nitrogen, R134a, R236fa, R245fa, R1234ze(E)	Bubble-Slug: 0.25-2.2 Slug-Churn: 0.5-3.04 Churn-Annular: 0.4-5.5	Adiabatic/ indirect diabatic

Table III presents the thermophysical properties of the fluids at saturation contained in the used databank. It can be seen that the refrigerants and hydrofluoroethers (HFE's) have fairly similar thermophysical properties in comparison to the difference in properties between deionised (DI) water and the other fluids, particularly the surface tension and vapour density.

TABLE III. SATURATED FLUID THERMOPHYSICAL PROPERTIES

Fluid	Surface Tension (σ) ($Nm^{-1} \times 10^{-3}$)	Vapour Density (ρ_g) (kgm^{-3})	Liquid Density (ρ_l) (kgm^{-3})	Vapour Viscosity (μ_g) ($kgm^{-1}s^{-1} \times 10^{-6}$)	Liquid Viscosity (μ_l) ($kgm^{-1}s^{-1} \times 10^{-3}$)
DI Water @ 1 bar	59.0	0.59	958.6	12.26	282.9
R134a @ 1 bar	8.5	29.16	1220	11.81	202.9
R245fa @ 1.85 bar	12.8	10.56	1321	10.40	372.8
HFE7100 @ 1 bar	9.6	9.52	1420	19.84	393.8
HFE7200 @ 1 bar	9.6	9.72	1303	12.19	355.9

The MAE% for the bubble to slug transitions are displayed in Table IV. If the prevailing flow pattern was correctly predicted by the correlation then the error of that data point was classified as 0%. However, if the flow pattern of the data point was incorrectly predicted then the percentage error was calculated for that point. Equation (3) was then used to calculate the MAE% for the entire data set. Whilst this is a useful parameter to understand which correlations may have performed well for one fluid, it is not useful to cross examine between fluids. This is due to the fact that models that significantly underpredict transition superficial gas velocities would appear to perform better than models that overpredict liquid superficial gas velocities. Therefore, the plots of the data and the predictions given by the correlations were also used when assessing each correlation.

$$MAE = \frac{100\%}{n} \sum \left| \frac{Ugs_{act} - Ugs_{pred}}{Ugs_{act}} \right| \quad (3)$$

The MAE% of correlations for the data containing R134a appears high. However, it can be seen in fig. 7, which presents the flow pattern map for R134a at 6 bar in a 1.1 mm vertical cylindrical tube, that this is due to the correlations overpredicting the superficial gas velocity for transition. If this is compared to the flow pattern map displayed in fig. 8, which depicts the correlations and data for DI water at 1 bar in a 1.1

This article has been accepted for publication in a future proceedings of this conference, but has not been fully edited. Content may change prior to final publication. Citation information: DOI 10.1109THERMINICXXXXX.2022.XXXXXXX, 2022 28th International Workshop on Thermal Investigations of ICs and Systems (THERMINIC))

mm hydraulic diameter rectangular channel, the correlations appear to predict the flow pattern transitions significantly better for R134a than for DI water despite the MAE% being considerably higher for R134a.

TABLE IV. MAE% OF BUBBLE TO SLUG CORRELATIONS

Fluid	DI Water @ 1 bar	R134a @ 6 bar	R245fa @ 1.85 bar	HFE7100 @ 1 bar	HFE7200 @ 1 bar
Chen et al.	38.5%	0.6%	39.4%	59.2%	56.1%
Mahmoud and Karayiannis	25.6%	120.4%	14.0%	41.6%	46.3%
Revellin and Thome	0%	138.71%	0.2%	4.3%	6.4%
Ong and Thome	33.3%	43.5%	37.4%	37.7%	42.7%
Tibiriçá et al.	40.0%	89.43%	0%	46.0%	48%

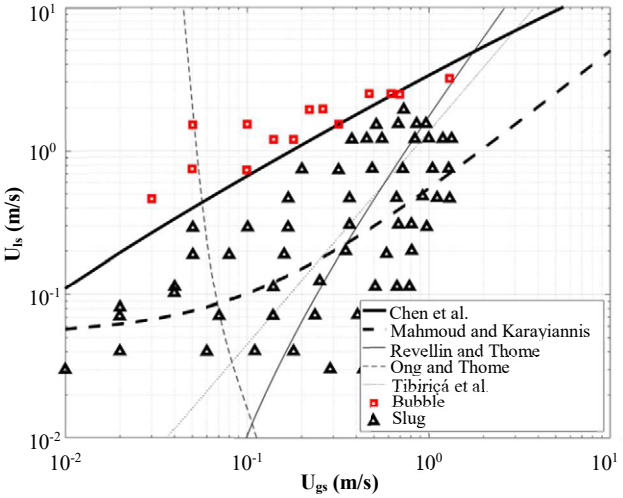

Fig. 7. Bubble to slug transitions for R134a @ 6 bar in a 1.1 mm hydraulic diameter circular channel

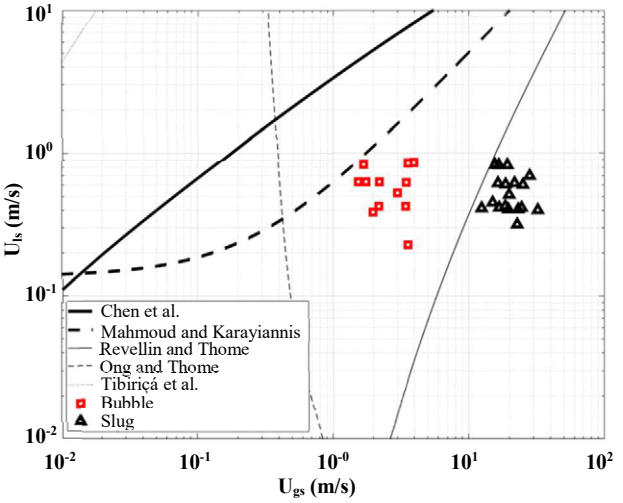

Fig. 8. Bubble to slug transitions for DI Water @ 1 bar in a 1.1 mm hydraulic diameter rectangular channel.

The model presented by Revellin and Thome performed well (with the exception of R134a). The correlation was able to capture more accurately the higher superficial gas velocities at which bubble to slug transitions occurs in water in comparison to the refrigerants and HFEs. The transition occurs at higher superficial gas velocities, but also at lower vapour qualities. The increased superficial gas velocities are a result of the notable decrease in vapour density in comparison to the other fluids. An explanation for the lower vapour quality at which the transition occurs in water may also be due to the increased surface tension of water. Equation (4) presents the Fritz [29] correlation for bubble departure diameter in subcooled flow boiling, where the diameter depends on $\sigma^{1/2}$. This increased departure diameter with surface tension will cause the bubble to depart at a large diameter, resulting directly or through coalescence with other large bubbles to slug flow at lower vapour qualities compared to lower surface tension fluids.

$$D_d = 0.0208\theta\sqrt{\sigma/[g(\rho_l - \rho_g)]} \quad (4)$$

The surface tension force therefore is important in flow regime transition in flow boiling. However only the correlations by Mahmoud and Karayiannis, Revellin and Thome and Ong and Thome consider it. It can be seen that the correlations by Mahmoud and Karayiannis and Ong and Thome underpredict the transition in water, which may be a result of the significantly reduced vapour density, i.e. greater specific volume, which is driving the transition to occur at higher superficial gas velocities for a given vapour quality. The gas only Weber number, which represents the ratio of vapour inertia forces to surface tension forces, is a parameter that captures both thermophysical properties. The correlation presented by Revellin and Thome, see below in (5), is the only one of the analysed correlations to utilise it, which indicates that it may be an important parameter in determining the transition from bubble to slug flows.

$$x = 0.763(Re_{lo}Bo/We_{go})^{0.41} \quad (5)$$

A final comment on the bubble to slug transition models, is that the trends of the correlations themselves are significantly different. This is even true for the correlations of Revellin and Thome, Mahmoud and Karayiannis and Chen et al., which all used similar fluids to formulate the data bases upon which their correlations were formulated. This may reflect the problem of subjectivity in defining flow patterns and the lack of clear universal definitions for how the transitions occur.

Table V presents the MAE% values for the transition between slug and churn flow. The flow pattern models of Revellin and Thome and Ong and Thome do not account for a transition to churn flow due to the designation of flow regimes. Thus, only two slug to churn models have been analysed. Despite there being clear phenomenological differences of the liquid-vapour interfaces in churn flow to slug or annular flow, there are few transition correlations that have been developed using diabatic experiments. The two correlations that have been analysed in this study perform well, except for DI water flows where the performance is less accurate.

TABLE V. MAE% OF SLUG TO CHURN CORRELATIONS

Fluid	DI Water @ 1 bar	R134a @ 6 bar	R245fa @ 1.85 bar	HFE7100 @ 1 bar	HFE7200 @ 1 bar
Chen et al.	40.0%	0.6%	2.8%	5.6%	7.1%
Tibiriçá et al.	25.8%	3.8%	5.0%	4.0%	7.8%

The churn to annular correlation provided by Chen et al. was based on three different mechanisms occurring, namely: (1) bubble elongation causing the surface tension force to become insufficient, thus distorting the interface (2) distortion of the slug nose or tail due to increased superficial gas

This article has been accepted for publication in a future proceedings of this conference, but has not been fully edited. Content may change prior to final publication. Citation information: DOI 10.1109THERMINICXXXXX.2022.XXXXXXX, 2022 28th International Workshop on Thermal Investigations of ICs and Systems (THERMINIC))

velocities at the nose or tail and (3) high liquid velocities distorting the vapour slug. Consequently, three empirical fits were made to describe these phenomena which are displayed in fig. 9.Conversely, Tibiriçá et al. developed their correlation through the use of a data bank with multiple fluids, multivariable statistical fitting with no relation to the physical mechanisms. This is true for all correlations by Tibiriçá et al. used in this study. An interesting feature of the two correlations is that the trends are very similar to each other with the Chen et al. correlation that describes the slug collapsing due to elongation of the bubble. This may infer that the problem of subjectivity in determining churn flow from slug flow is not so prevalent, i.e. the transition is quite a sudden process and therefore, easier to determine a clear parametric point at which the transition occurs.

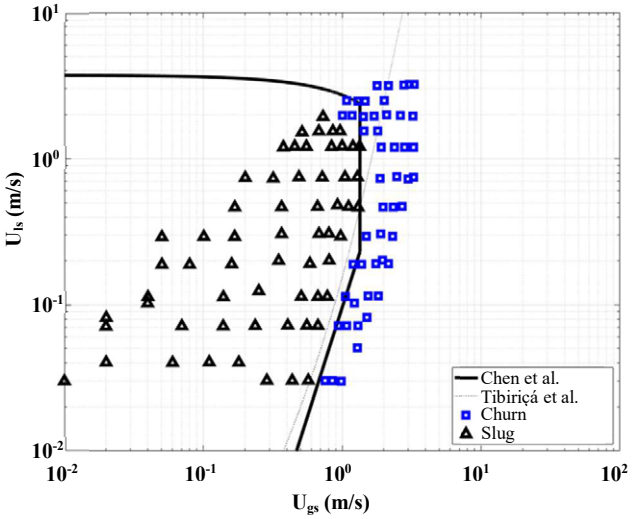

Fig. 9. Slug to churn transitions for R134a @ 6 bar in a 1.1 mm hydraulic diameter circular channel

Once again, the correlations did not perform well for the flows that use water. As both correlations were based primarily on empirical statistical fits, albeit with Chen et al. explaining the mechanisms, the reason for poor performance can be seen in Table I, which presents the fluids that were used in each data bank to develop the correlations. The Chen et al. correlation was obtained using only R134a data and the Tibiriçá et al. analysis was conducted primarily for refrigerants and nitrogen. The use of nitrogen and the associated difference in thermophysical properties to typical refrigerants will have provided some inclusion of the thermophysical properties into the best statistical fit. However solely including nitrogen was insufficient to fully capture the effects of thermophysical properties, such as the increased surface tension and decreased vapour density, in the correlation. Thus, if a universal flow pattern map is to be developed for microscale flows a large databank containing many geometries, flow parameters and fluids of significantly varying thermophysical properties must be used.

Table VI. displays the MAE% percentage of the churn to annular flow pattern prediction models. Once again, the correlations appear to perform quite well, with the exception of the water data. Fig. 10 shows the flow pattern correlations for churn to annular flows for HFE7100 at 1 bar in a 0.6 mm hydraulic diameter rectangular horizontal channel. It can be seen that the trends for all correlations are fairly similar. This indicates that the churn to annular transition does not suffer from the issues of subjectivity and that the method of measuring bubble count frequency is comparable to visual observations.

TABLE VI. MAE% OF CHURN TO ANNULAR CORRELATIONS

Fluid	DI Water @ 1 bar	R134a @ 6 bar	R245fa @ 1.85 bar	HFE7100 @ 1 bar	HFE7200 @ 1 bar
Chen et al.	18.7%	2.8%	16.8%	4.7%	0.3%
Revellin and Thome	482.6%	24.3%	18.5%	6.9%	0.15%
Ong and Thome	0%	7.7%	5.9%	10.7%	2.5%
Tibiriçá et al.	21.1%	0.03%	8.6%	4.7%	0.1%

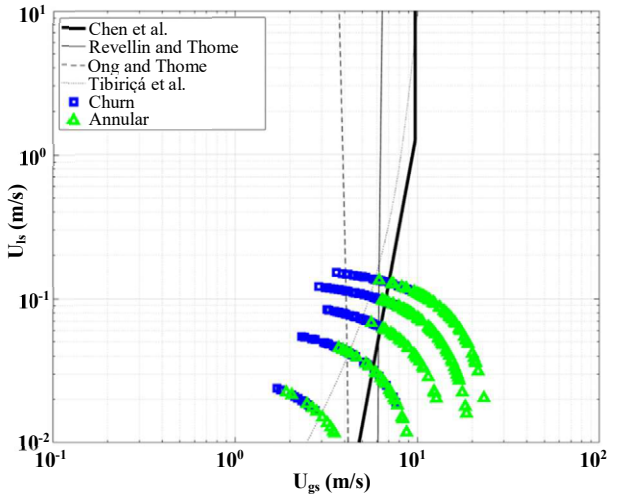

Fig. 10. Churn to annular transitions for HFE7100 @ 1 bar in a 0.46 mm hydraulic diameter rectangular channel

The prediction models perform fairly well for the DI water data with the exception of the correlation presented by Revellin and Thome, unlike the bubble to slug and slug to churn transitions. The correlations presented by Chen et al.in (6) and (7), show a dependence of the transition on the liquid Weber number, the gas Froude number and the gas Reynolds number. The gas Froude number is an interesting inclusion as it represents the ratio of inertial to buoyancy forces. The transition criterion provided by Ong and Thome includes the confinement number, which considers the suppression of the buoyancy forces in relation to the surface tension forces. The correlation provided by Tibiriçá et al. also includes a variation of the Froude number, thus also considering the buoyancy forces. The correlation that did not consider the effect of buoyancy forces, which for a given volume of vapour for water is significantly larger than for refrigerants, was that of Revellin and Thome. The correlations imply that suppression of the buoyancy force in relation to the other forces results in a faster transition to churn flow.

$$We_{ls} = 1.567 \times 10^{-17} (Fr_{gs} Re_{gs})^{3.41} \quad (6)$$

$$Fr_{gs} Re_{gs} = 3.119 \times 10^{5} \quad (7)$$

IV. CONCLUSIONS AND RECOMMENDATIONS

A discussion of the flow patterns in the conventional scale was presented, which included the flow patterns of stratified, bubble, annular and intermittent (elongated bubble, confined bubble, slug and churn) flows. Reports of an absence of stratified flow was explained through the scaling of forces that act on the liquid vapour interface and the weaker effect of the buoyancy force, particularly in reference to the surface tension force. Subsequently, a qualitative definition of the microscale was provided in which the microscale occurs at hydraulic

This article has been accepted for publication in a future proceedings of this conference, but has not been fully edited. Content may change prior to final publication. Citation information: DOI 10.1109THERMINICXXXXX.2022.XXXXXXX, 2022 28th International Workshop on Thermal Investigations of ICs and Systems (THERMINIC)

diameters low enough such that stratified flow cannot exist in horizontal channels. A brief overview of the terminology and classifications of flow patterns in the microscale was presented and the associated challenges of a lack of universal terminology and subjectivity in determining flow patterns considered. It is recommended that the global heat transfer community adopt the generic flow pattern designations of bubble, slug, churn and annular flows to eliminate the problem of subjectivity and to allow for universal terminology. This is not to suggest that the subdivision of flow patterns is not beneficial, however a full understanding and ability to predict the generic categorisations must be achieved first.

Finally, a data bank of two-phase microchannel flows containing over 1500 data points was compared to existing flow pattern prediction models. The results found that there may exist significant problems of subjectivity in determining the bubble to slug transitions, whilst this difficulty did not appear present in the slug to churn and churn to annular transitions. The inability to predict the transitions of bubble to slug and slug to churn for water shows that a large data bank containing many geometries, flow parameters and fluids with varying thermophysical properties will be required to develop a successful universal flow pattern map in the microscale. Additionally, the gas Weber number was found to potentially be an important parameter in the prediction of the bubble to slug transition. The relatively weaker buoyancy forces were also found to result in an early transition between churn and annular flows.

The comparison of our data with the available correlations in literature indicates that the correlations recommended by Chen et al. Mahmoud and Karayiannis, Ong and Thome, Revellin and Thome and Tibiriçá et al. could be considered further in subsequent analysis.

ACKNOWLEDGEMENT

The project is supported by the Engineering and Physical Sciences Research Council of the UK under grant EP/T033045/1.

REFERENCES

[1] J. Gao, Z. Hu, Q. Yang, X. Liang, and H. Wu, “Fluid flow and heat transfer in microchannel heat sinks: Modelling Review and Recent Progress:,” *Thermal Science and Engineering Progress*, Vol. 29, Mar. 2022.

[2] S. Wang, D. Zhou, and Z. Yang, “Design of a cooling system for microchips with high heat-flux density using integrated microchannels,” *Heat Transfer Research*, vol. 48, no. 14, pp. 1299–1312, 2017.

[3] B. Allard, C. Buttay, C. Martin and H. Morel, “Considerations for High Temperature Power Electronics.”, *18th International Symposium on Power Electronics Ee2015*, Oct. 2015.

[4] E. M. Fayyadh, M. M. Mahmoud, K. Sefiane, and T. G. Karayiannis, “Flow boiling heat transfer of R134a in multi microchannels,” *International Journal of Heat and Mass Transfer*, vol. 110, pp. 422–436, Jul. 2017.

[5] T. G. Karayiannis and M. M. Mahmoud, “Flow boiling in microchannels: Fundamentals and applications,” *Applied Thermal Engineering*, vol. 115, pp. 1372–1397, Mar. 2017.

[6] Y. Wang and K. Sefiane, “Effects of heat flux, vapour quality, channel hydraulic diameter on flow boiling heat transfer in variable aspect ratio micro-channels using transparent heating,” *International Journal of Heat and Mass Transfer*, vol. 55, no. 9–10, pp. 2235–2243, Apr. 2012.

[7] Y. Li, G. Xia, Y. Jia, Y. Cheng, and J. Wang, “Experimental investigation of flow boiling performance in microchannels with and without triangular cavities – A comparative study,” *International Journal of Heat and Mass Transfer*, vol. 108, pp. 1511–1526, May 2017.

[8] M. M. Mahmoud and T. G. Karayiannis, “Flow pattern transition models and correlations for flow boiling in mini-tubes,” *Experimental Thermal and Fluid Science*, vol. 70, pp. 270–282, Jan. 2016.

[9] C. L. Ong and J. R. Thome, “Macro-to-microchannel transition in two-phase flow: Part 1 - Two-phase flow patterns and film thickness measurements,” *Experimental Thermal and Fluid Science*, vol. 35, no. 1, pp. 37–47, Jan. 2011.

[10] J. R. Thome and A. Cioncolini, “Two-Phase Flow Pattern Maps for Microchannels,” 2015.

[11] J. R. Thome, A. Bar-Cohen, R. Revellin, and I. Zun, “Unified mechanistic multiscale mapping of two-phase flow patterns in microchannels,” *Experimental Thermal and Fluid Science*, vol. 44, pp. 1–22, Jan. 2013.

[12] S. G. Kandlikar, “Scale effects on flow boiling heat transfer in microchannels: A fundamental perspective,” *International Journal of Thermal Sciences*, vol. 49, no. 7, pp. 1073–1085, Jul. 2010.

[13] Y. Taitel, “Flow pattern transition in two phase flow,” in *9th International Heat Transfer Conference*, Aug. 1990.

[14] V. Y. S. Lee and T. G. Karayiannis, “Effect of inlet subcooling on flow boiling in microchannels,” *Applied Thermal Engineering*, vol. 181, p. 115966, Nov. 2020.

[15] A. H. Al-Zaidi, M. M. Mahmoud, and T. G. Karayiannis, “Effect of aspect ratio on flow boiling characteristics in microchannels,” *International Journal of Heat and Mass Transfer*, vol. 164, p. 120587, 2021

[16] V. Y. S. Lee, A. Al-Zaidi, G. Henderson, and T. G. Karayiannis, “Flow Boiling Results of HFE-7200 in a Multi-Microchannel Evaporator and Comparison with HFE-7100,” Apr. 2019.

[17] A. H. Al-Zaidi, M. M. Mahmoud, and T. G. Karayiannis, “Flow boiling of HFE-7100 in microchannels: Experimental study and comparison with correlations,” *International Journal of Heat and Mass Transfer*, vol. 140, pp. 100–128, Sep. 2019.

[18] L. Chen, Y. S. Tian, and T. G. Karayiannis, “The effect of tube diameter on vertical two-phase flow regimes in small tubes,” *International Journal of Heat and Mass Transfer*, vol. 49, no. 21–22, pp. 4220–4230, Oct. 2006.

[19] T. C. Thulasidas, M. A. Abraham, and R. L. Cerro, “Flow patterns in liquid slugs during bubble-train flow inside capillaries,” *Chemical Engineering Science*, vol. 52, no. 17, pp. 2947–2962, Sep. 1997.

[20] C. A. Damianides and J. W. Westwater, “Two-phase Flow Patterns in a Compact Heat Exchanger and in Small Tubes,” 1988.

[21] J. W. Coleman and S. Garimella, “Characterization of two-phase flow patterns in small diameter round and rectangular tubes,” *International Journal of Heat and Mass Transfer*, vol. 42, no. 15, pp. 2869–2881, Aug. 1999.

[22] Y. Fan, E. Al-Safran, E. Pereyra, and C. Sarica, “Modeling pseudo-slugs liquid holdup in slightly upward inclined pipes,” *Journal of Petroleum Science and Engineering*, vol. 194, p. 107564, Nov. 2020.

[23] M. Habibi Matin and S. Moghaddam, “Mechanism of transition from elongated bubbles to wavy-annular regime in flow boiling through microchannels,” *International Journal of Heat and Mass Transfer*, vol. 176, p. 121464, Sep. 2021.

[24] R. Revellin and J. R. Thome, “A new type of diabatic flow pattern map for boiling heat transfer in microchannels,” in *Journal of Micromechanics and Microengineering*, Apr. 2007.

[25] E. Costa-Patry, J. Olivier, and J. R. Thome, “Heat transfer charcacteristics in a copper micro-evaporator and flowpattern-based prediction method for flowboiling in microchannels,” *Frontiers in Heat and Mass Transfer*, vol. 3, no. 1, 2012.

[26] J. R. Thome, V. Dupont, and A. M. Jacobi, “Heat transfer model for evaporation in microchannels. Part I: presentation of the model,” *International Journal of Heat and Mass Transfer*, vol. 47, no. 14–16, pp. 3375–3385, Jul. 2004.

[27] Y. F. Li, G. D. Xia, D. D. Ma, J. L. Yang, and W. Li, “Experimental investigation of flow boiling characteristics in microchannel with triangular cavities and rectangular fins,” *International Journal of Heat and Mass Transfer*, vol. 148, p. 119036, Feb. 2020.

[28] C. Tibiriçá, D. Rocha, I. Sueth Jr., G. Bochio, G. Shimizu, M. Barbosa and S. Ferreira, “A complete set of simple and optimized correlations for microchannel flow boiling and two-phase flow applications,” *Applied Thermal Engineering*, vol. 126, pp. 774–795, Nov. 2017.

[29] W. Fritz, “The calculation of the maximum volume of steam bladders,” *Phys. Z*, vol. 36, pp. 379–384,